

SATELLITE OBSERVATION OF SURFACE ALBEDO OVER THE QINGHAI-XIZANG PLATEAU REGION

Zhong Qiang (钟强) and Li Yinhai (李银海)

Lanzhou Institute of Plateau Atmospheric Physics,

Academia Sinica, Lanzhou

Received September 19, 1986

ABSTRACT

A method has been developed to determine the surface albedo over the Qinghai-Xizang Plateau region from NOAA polar orbiter AVHRR (Advanced Very High Resolution Radiometer) data. The empirical relationship between clear-sky planetary and surface albedos is established the basis of surface global radiation measurements and the specified ratio between atmospheric reflection and absorption of solar radiation. The method is applied to the Qinghai-Xizang region with several measurements during the period of Sep. to Nov., 1985. A comparison is presented between the estimated surface albedos and that of surface observation. The results show that the presented method is suitable to detecting the spatial and temporal variation of surface albedo and is relevant for climatological studies. The possible error sources and improvements are discussed as well.

I. INTRODUCTION

Surface albedo is an important parameter for radiation budget calculation and climate modelling. Satellites appear to be the best existing tools for deriving surface albedo maps at the climatic scale even though there will be various difficulties encountered in the use of satellite measurements. Some works have been published with METEOSAT and SMS-1 geosynchronous satellite data on surface albedo over Africa's Sahara Desert region (Rockwood et al., 1978; Pinty et al., 1985a, b). The Qinghai-Xizang Plateau is one of the climatically sensitive regions. Owing to its complicative topography and the scarcity of surface observation stations, the application of satellite observations is bound to be helpful to understand the characteristics of surface albedo over this region.

In this paper, the method to determine the surface albedo over the Qinghai-Xizang Plateau region from NOAA polar orbiter AVHRR data is investigated. Several measurements obtained from the period of Sep. to Nov., 1985 are analysed and some discussions are given about the possible error sources and the way for improvement.

II. METHOD AND EVALUATION PROCEDURES

The data used in this work are AVHRR data. Because AVHRR measures the reflected and scattered solar radiation at the top of atmosphere with narrow-band (NB) and narrow-field of view (NFOV), the climatic scale surface albedo derived from these measurements must take the following computational steps into account. These steps are

1. Deriving of the Spectral Albedos of Visible and Near-Infrared Channels from AVHRR Data

The visible and near-infrared channel data (channel 1: 0.58–0.68 micron and channel 2: 0.725–1.1 micron) can be converted into spectral albedos α_i ($i=1, 2$) respectively with a calibration technique (Lauritson, 1979) and taking account of the solar zenith correction:

$$\alpha_i = (S_i C_i + I_i) / \cos \xi, \quad (1)$$

where C is the measured radiance in counts and S and I are calibration coefficients. i is the channel number, and ξ is the solar zenith angle.

2. Anisotropic Correction for the Dependence of the Measured Values on the Viewing Angle and Relative Azimuthal Angle of Measurements

The anisotropic correction equation is

$$\alpha_i^* = \alpha_i \cdot X(\xi, \theta, \psi), \quad (2)$$

where X is the correction function which is related to the solar zenith angle, viewing angle θ and relative azimuthal angle ψ of measurement. In this study, the angular reflectance models defined by Raschke et al. (1973) are used.

3. Transformation from the Narrow Bands to the Total Solar Spectrum

The following multiple regression equation obtained from the radiative transfer calculation for the Plateau model atmospheres with various conditions of surface albedo and surface elevation is adopted for this transformation (Zhong et al., 1985).

$$\alpha_p = A + \sum_{n=1}^3 B_n (\alpha_i^*)^n + \sum_{n=1}^3 C_n (\alpha_i^*)^n, \quad (3)$$

where A , B_n , C_n are regression coefficients depending on solar zenith angle ξ . In Table 1 these regression coefficients are summarized for different values of ξ . The multiple correlation coefficient m and the standard error σ are also given.

In order to assess the error of calculated albedo caused by using the regression coefficients derived from model atmospheres to realistic ones, we make some comparing tests for random sampling to calculate α_p with Eq. (3) and with the summer's and winter's coefficients respectively for the same measurement data. It is shown that the resulted differences are less than 0.001. This means that the uncertainties inherent in the model atmospheres from which the coefficients were derived would not affect significantly the availability of the coefficients.

Table 1. Regression Coefficients, Standard Error σ and Multiple Correlation Coefficient m (ξ =Solar Zenith Angle)

a. Summer

| ξ | A | B_1 | B_2 | C_1 | C_2 | C_3 | σ | m |
|-------|---------|--------|--------|--------|---------|--------|----------|---------|
| 25° | -0.0006 | 0.3460 | 0.1141 | 0.6131 | -0.1853 | 0.1290 | 0.00245 | 0.99989 |
| 35° | 0.0014 | 0.3360 | 0.1212 | 0.6066 | -0.1581 | 0.1079 | 0.00246 | 0.99989 |
| 45° | 0.0025 | 0.3143 | 0.1523 | 0.6236 | -0.1845 | 0.1026 | 0.00228 | 0.99990 |
| 55° | 0.0037 | 0.2866 | 0.1803 | 0.6487 | -0.2167 | 0.1083 | 0.00212 | 0.99991 |
| 65° | 0.0086 | 0.2622 | 0.1946 | 0.6424 | -0.1727 | 0.0771 | 0.00189 | 0.99991 |

b. Winter

| ξ | A | B_1 | B_2 | C_1 | C_2 | C_3 | σ | m |
|-------|--------|--------|--------|--------|---------|--------|----------|---------|
| 25° | 0.0008 | 0.3332 | 0.1354 | 0.6159 | -0.1693 | 0.0901 | 0.00332 | 0.99982 |
| 35° | 0.0016 | 0.3205 | 0.1494 | 0.6236 | -0.1791 | 0.0931 | 0.00283 | 0.99987 |
| 45° | 0.0023 | 0.2958 | 0.1780 | 0.6480 | -0.2236 | 0.1127 | 0.00278 | 0.99986 |
| 55° | 0.0044 | 0.2913 | 0.1731 | 0.6408 | -0.2036 | 0.1129 | 0.00249 | 0.99988 |
| 65° | 0.0079 | 0.2620 | 0.1920 | 0.6564 | -0.2182 | 0.1264 | 0.00220 | 0.99989 |

4. Determination of the Clear-Sky Planetary Albedo

The albedo α_p obtained from steps 1-3 is that at the top of atmosphere (TOA), i.e. the planetary albedo. In order to get the surface albedo it is necessary to get the clear-sky planetary albedo by eliminating the cloud contamination. It is known from the experience based on surface observations and satellite images that the clouds are more frequent over the Qinghai-Xizang Plateau region in the midafternoon when the NOAA daytime satellite takes observations. The contamination of cloud will seriously affect the estimated surface albedo (overestimating the surface albedo). After comparing various threshold methods we choose the visible criterion $\alpha_v^* > 0.35$ as the index of cloud. This threshold value allows us to filter the high reflectivity value of cloud and avoid filtering that of desert. In the computation program, the elimination of cloud is executed for each pixel before step 3 and therefore Eq. (3) gives the clear-sky planetary albedo.

5. Determination of Surface Albedo

For an arbitrary atmospheric column, the solar radiation budget equation is

$$Q_a = Q_0(1 - \alpha_p) - Q_s(1 - \alpha_s), \quad (4)$$

where α_s is the surface albedo, Q_0 is the insolation (incoming shortwave flux) at the top of atmosphere, Q_s is global radiation (surface insolation) and Q_a is the solar radiation absorbed by the atmosphere.

The relationship between clear-sky planetary albedo and surface albedo can be derived when we apply Eq. (4) to the clear-sky. That is:

$$\alpha_p = a\alpha_s + b, \quad (5)$$

where $a = Q_s/Q_0$ representing the total transmittance of clear-sky atmosphere and $b = 1 - (Q_s - Q_a)/Q_0$ representing the reflectance of clear-sky atmosphere resulting from the backward scattering of molecule and aerosol.

The determination of coefficients a and b is crucial for relationship (5). They can be determined based on radiation transfer modeling simulations (Preuss et al., 1980; Chen et al., 1984; Zhong et al., 1985). But the determination of a and b in this way may encounter difficulties because of the lack of data on aerosol optical properties, in particular, for high solar zenith angle. In this study, instead of modeling simulations, we determine the coefficient a in Eq. (5) based on the surface global radiation observation data and b with giving a specified ratio of atmospheric reflectance to absorption. Based on the surface global radiation observation in clear-sky during the period of Qinghai-Xizang Plateau Field Experiment (Aug., 1982—July, 1983), we obtained the relationships between the clear-sky global radiation Q_s and the solar zenith angle for different observation stations with different elevations (Zhong, 1986), and an empirical relationship was derived between the ratio $a = Q_s/Q_0$ and the surface

elevation (km) for different solar zenith angles. That is

$$a = 1 - (1 - a_0)e^{-K \cdot z^2}, \quad (6)$$

where K and a_0 (the value of a at $z=0$) are parameters depending on solar zenith angle. Their values are listed in Table 2.

Table 2. Parameters a_0 and K in Eq. (6)

| ζ (deg.) | 5 | 15 | 25 | 35 | 45 | 55 | 65 | 75 |
|----------------|-------|-------|-------|-------|-------|-------|-------|-------|
| a_0 | 0.733 | 0.731 | 0.727 | 0.721 | 0.713 | 0.697 | 0.675 | 0.630 |
| K | 0.032 | 0.031 | 0.030 | 0.028 | 0.026 | 0.023 | 0.018 | 0.012 |

In order to determine the value of b from Eq. (4) and the definition of b , we need the simultaneous measurements of α_p , α_s and Q_s . Because there are no necessary data available, we adopt the following method.

We define $f = b/(1-a)$ representative of the ratio of the reflective radiation Q_r caused by backward scattering of molecule and aerosol to the total extinction of solar radiation ($Q_0 - Q_s$) in dust sky. Because the aerosol has the absorbing and scattering effects simultaneously, the decreasing (increasing) of the value a with change in aerosol would be combined by the increasing (decreasing) of the value b and then the ratio f is relatively stable. Therefore, the coefficient b can be defined as

$$b = (1-a) \cdot f. \quad (7)$$

Chen and Ohring (1984) obtained $f = 0.22$ with the radiation model by Lacis and Hansen (1974). Because the model does not include the effects of aerosol, it is reasonable to expect that the value f is somewhat greater than this in dust sky. According to the study by Preuss and Geleyn (1980), $f = 0.25$ for global average and it is used in this study.

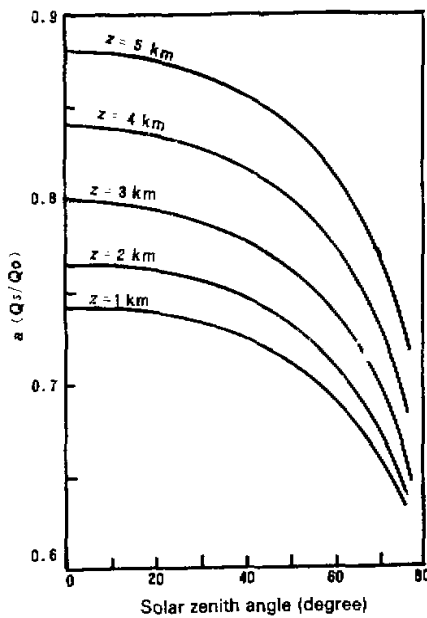


Fig. 1 Parameter a as function of solar zenith angle for different surface elevations Z .

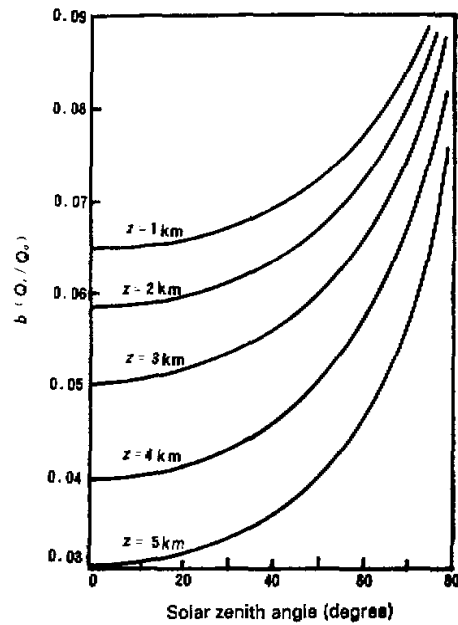


Fig. 2 Parameter b as function of solar zenith angle for different surface elevations Z .

Taking into account the solar zenith dependence of value f , there will be certain error for adopting a fixed value f . The solar zenith angle ranges from about 40° to 70° in the midafternoon when the NOAA daytime satellite passes. Assuming the corresponding change in the value f ranges from 0.21 to 0.29 (and let $a=0.7$), the resulted error of b for neglecting the solar zenith dependence of f does not exceed ± 0.015 and it satisfies the accuracy requirement of the surface albedo in climatological study.

The functions of a and b are presented graphically in Fig. 1 and Fig. 2 respectively. Once the coefficients a and b are determined for a given solar zenith angle and a surface elevation, the surface albedo can be derived from planetary albedo with Eq. (5).

III. RESULTS

The albedo maps presented in Fig. 3 are derived from the selected AVHRR measurements with clear or lightly cloudy sky over the related region during the period of Sep. to Nov., 1985. The scanning times are at approximately 15:00 Local Solar Time (LST). The data were received at TIROS-N/NOAA Satellite Data Receiving Station, Satellite Meteorology Center, Beijing, China. In order to get the average albedo over an area relevant for climate study, the results are averaged in spatial scale $2^\circ \times 2^\circ$. Further, since α_s varies strongly with the solar zenith angle, especially at higher zenith angles, for the same measurement case each measuring point has a different solar zenith angle because of their different locations. Empirical Eq. (8) (Paltridge et al., 1976) is used for getting normalized α_s .

$$\alpha_s(\xi) = \alpha_0 + (1 - \alpha_0)e^{-\lambda(90^\circ - \xi)}, \quad (8)$$

Empirical coefficient λ is 0.14. The albedo α_0 at high solar elevation is determined by $\alpha_s(\xi)$ and ξ for each grid square with Eq. (8). Then α_s is normalized with Eq. (8) again to the value

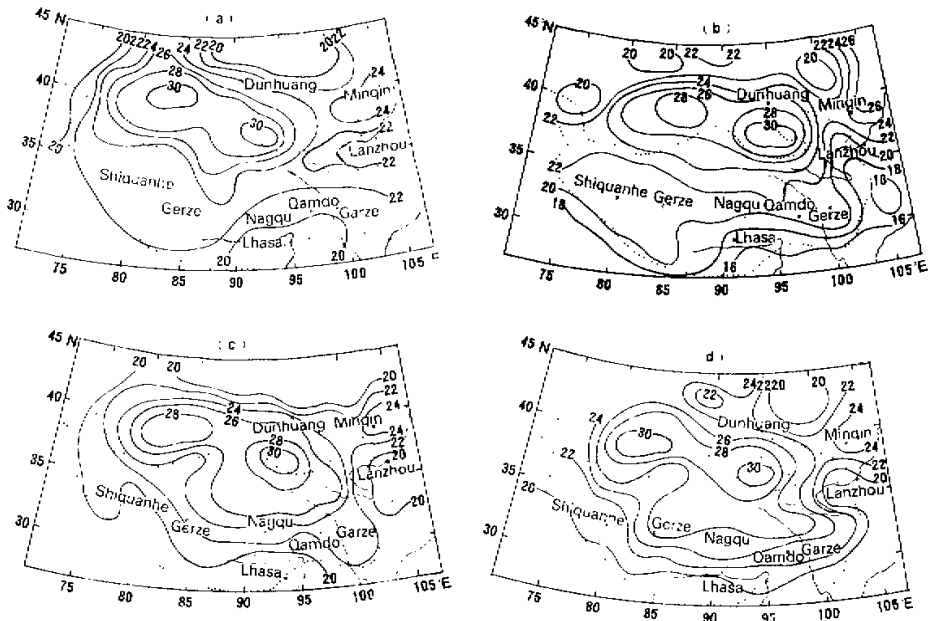


Fig. 3 Satellite derived the surface albedo (percent) from AVHRR data in 1985.

(a) Sep. 23, (b) Oct. 4, (c) Oct. 31, (d) Nov. 19.

$\alpha_s(\bar{\zeta})$ corresponding to the monthly mean solar zenith angle at the related latitude.

The results show that the surface albedo in the desert area of Tarim Basin and Qaidam Basin may reach 0.30, and about 0.18-0.28 for Plateau region. Affected by the precipitation (change in soil moisture), the surface albedo for the same area appears to have distinct temporal variation. For example, there is a heavier precipitation process in the Sichuan-Xizang region from Sep. 25 to Oct. 2, 1985. Figure 4 is the precipitation map for the last ten days of September, 1985. Comparing the albedo maps of Sep. 23 and of Oct. 4, the albedo over most part of the Plateau region decreases obviously after the precipitation process. This fact indicates that the surface albedo is very sensitive to the soil moisture status related to the precipitation and the change in surface albedo can be detected by the satellite scanning.

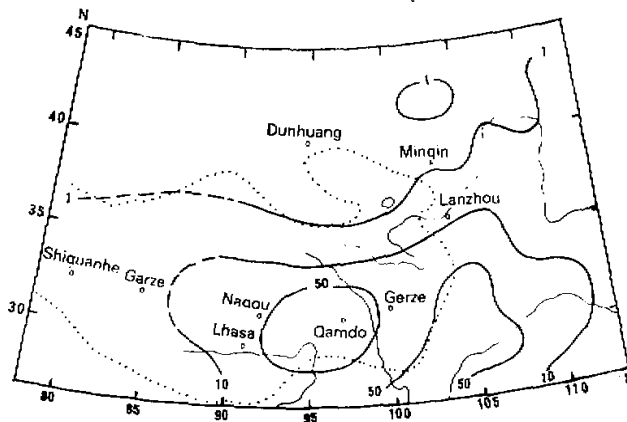


Fig. 4. Rainfall amount (mm) of the last ten days of Sep., 1985.

Table 3 presents a comparison between the satellite observations of Sep. 23, Oct. 31 and Nov. 19 mentioned above and the surface observations in the corresponding month, 1982. The former is the average value in the area of $2^\circ \times 2^\circ$ grid square in which the station is located.

Table 3. Comparison between Surface Albedos Derived from Satellite and that from Ground Measurement

| Station | Height (m) | Sep. | | Oct. | | Nov. | |
|-----------|---------------|------|------|------|------|------|------|
| | | I | II | I | II | I | II |
| Shiquanhe | 4278 | 0.22 | 0.21 | 0.19 | 0.22 | 0.21 | 0.25 |
| Garze | 4415 | 0.23 | 0.25 | 0.24 | 0.27 | 0.27 | 0.29 |
| Nagqu | 4507 | 0.21 | 0.18 | 0.23 | 0.24 | 0.25 | 0.41 |
| Lhasa | 3659 | 0.19 | 0.19 | 0.20 | 0.20 | 0.22 | 0.22 |
| Qamdo | 3241 | 0.20 | 0.21 | 0.23 | 0.23 | 0.24 | 0.26 |
| Garze | 3394 | 0.21 | 0.16 | 0.22 | 0.19 | 0.23 | 0.21 |
| Lanzhou | 1518 | 0.21 | 0.17 | 0.19 | 0.19 | 0.20 | 0.21 |
| Mingjin | 1367 | 0.27 | 0.29 | 0.26 | 0.30 | 0.28 | 0.34 |
| Dunhuang | 1140 | 0.25 | 0.27 | 0.26 | 0.29 | 0.26 | 0.29 |

I Derived from satellite observations

II Monthly average of surface observations

The latter is the monthly average value of the surface albedo measurements. Owing to the different sampling in space and time, the comparison presented in Table 3 should not be considered as error estimation but as differences between the satellite-derived albedos and ground measurements. The comparison shows that the number of cases with absolute difference less than or equal to 0.03 accounts for 78% of the total cases, indicating a good agreement between the two kinds of measurements. There is a distinct difference in the case of November at Nagqu. The high monthly mean value of 0.41 resulted from having ten days' snow cover in that month at Nagqu. However, the satellite-derived value is for no snow cover, and it will be discussed in the next section.

IV. DISCUSSION

In this section, we will discuss two problems. One is about the source of errors and the other is about the snow cover.

(1) The time variations of derived surface albedo as shown in the different temporal samples of Fig. 3 are primarily the indication of changes in surface status, but may also result from various errors in the deriving procedures. The possible errors may be introduced by:

- A. the anisotropic property of the reflected radiation and the tilted surface;
- B. visible threshold being failing for very small and thin clouds; and
- C. the uncertainty of coefficients a and b in Eq. (5) caused by the variation of atmospheric state (in particular, the aerosol).

In order to overcome error source B , the contamination of small and thin clouds should be eliminated to permitted extent by composing the expected clear-sky samples.

Now we discuss error source C . The ratio $a = Q_p/Q_0$ depends on not only the solar zenith angle, surface elevation but also the atmospheric state. Empirical Eq. (5), derived on the basis of climatological data, is representative of the functional relation in the mean state (climatic state). According to Zhong (1986), the averaged standard error of the empirical fitted relationship between the global radiation in clear-sky and the solar zenith angle is about 26 W/m^2 for the Plateau region. Assuming $Q_0 = 1370 \text{ W/m}^2 \times \cos 60^\circ = 685 \text{ W/m}^2$, we can estimate that the probable change in value a is about ± 0.038 for the uncertainty of the atmospheric state. As pointed out in section II. 5, the decreasing (increasing) of the value a affected by aerosol is bound to be combined simultaneously by the increasing (decreasing) of the value b . Therefore, in the transformation between α_s and α_p using Eq. (5), the influence of aerosol on the value a would be compensated by the influence on the value b to a certain extent.

Based on the relationships of Eq. (5) and Eq. (7), we obtain

$$\alpha_p = (\alpha_s - f) \cdot a + f \quad (9)$$

or

$$\alpha_s = (\alpha_p - f) / a + f. \quad (9')$$

Eq. (9) indicates that when $\alpha_s = f$, α_p has the same value as α_s , ($\alpha_p = \alpha_s = f$). It means that the positive and negative effects of atmosphere on the albedo are compensated each other at this particular condition. The more the value of albedo closes to f , the less the influence of atmosphere will be.

The sensitivity of estimated albedo value to the error of coefficient a can be estimated with Eq. (9'). Differentiating Eq. (9') with respect to a , we obtain

$$\frac{\partial \alpha_s}{\partial a} = -\frac{\alpha_p - f}{a^2}. \quad (10)$$

Taking $f=0.25$, corresponding to $\alpha_p=0.2-0.3$, the error in the estimated surface albedo is the order of 0.01 respect to an error of 0.1 in coefficient a , that is, the estimated albedo is not very sensitive to the change in value of a , and Eq. (5) can reach the required accuracy of 0.02 for the surface albedo in climate monitor and modeling.

The more severe problem is the anisotropic property of reflective radiation and the undulate topography as the Plateau is. The NOAA daytime satellite takes observations in the mid-afternoon with high solar zenith angles. The measurements will be contaminated by shadows from mountains and it biases the observations toward the low albedo. In this study, the unrealistic low values are filtered as noise with near-infrared threshold $\alpha_i^* < 0.15$.

(2) Because the snow cover is similar to cloud in reflective property, the snow cover of high reflectance will be filtered simultaneously when the cloud is filtered. Thus the estimated surface albedo in this study means that for no snow cover. Taking account of the strong influence of snow cover on the surface albedo, and then the radiation budget, it is necessary in the view point of climate study to compose surface albedo maps in three grades according to different demands on spacial and temporal scale: A. Excluding snow cover, B. Including permanent snow cover, and C. Including permanent and non-permanent snow cover. And the scheme for distinguishing the snow cover from the cloud with the multiple-spectral method should be developed.

V. FINAL REMARKS

The relationship presented in this paper between clear-sky planetary and surface albedos enables one to estimate the surface albedo, given only the planetary albedo, and vice versa. The technique to determine the coefficients of this relationship based on the surface global radiation measurements can be applied to other climate regions. The relationship should also be suitable for use in simple climate models for parameterizing the clear-sky planetary albedo in terms of the surface albedo. The prior specified value of reflected solar radiation of pure atmosphere accounting for 1/4 of the total extinction should be validated with field experiments including simultaneous observations from satellites against ground truth. And the error analyses are required.

REFERENCES

- Chen, T.S. and Ohring, G. (1984), On the relationship between clear-sky planetary and surface albedos, *J. Atmos. Sci.*, **41**:156-158.
- Lacis, A.A. and Hansen, J.E. (1974), A parameterization for the absorption of solar radiation in the earth's atmosphere, *J. Atmos. Sci.*, **31**:118-133.
- Lauritson, L. (1979), NOAA-Technical Memorandum, NESS 107, Washington D.C., 46 pp.
- Paltridge, G.W. and Platt, C.M.R. (1976), Radiative processes in meteorology and climatology, Elsevier, New York, 133pp.
- Pinty, B., Szejwach, G. and Stum, J. (1985a), Surface albedo over the Sahel from METEOSAT Radiances, *J. Climate Appl. Meteor.*, **24**:108-113.
- Pinty, B. and Szejwach, G. (1985b), A new technique for inferring surface albedo from satellite observations, *J. Climate Appl. Meteor.*, **24**:741-750.
- Preuss, H.J. and Geleyn, J.F. (1980), Surface albedos derived from satellite data and their impact on forecast models, *Arch. Met. Geoph. Biokl., Ser. A*, **29**:345-356.
- Raschke, E., Vonder Harr, T.H., Pasternak, M. and Bandoen, W.R. (1973), The radiation balance of the earth-atmosphere system from Nimbus 3 radiation measurements, NASA TN D-7249, Washington D.C., pp. 10-13.
- Rockwood, A.A. and Cox, S.K. (1978), Satellite inferred surface albedo over northwestern Africa, *J. Atmos. Sci.*, **35**:513-522.

-
- Zhong Qiang and Wu shijie (1985), A method for determining surface albedo over the Tibetan Plateau from AVHRR data, *Plateau Meteorology*, **4**:193-203 (in Chinese with English abstract).
- Zhong Qiang (1986), Discussions in the climatological methods of calculating the global solar radiation over the Qinghai-Xizang Plateau area, *Plateau Meteorology*, **5**:197-210 (in Chinese with English abstract).

